Imaging Model of Missile-borne Linear Array Scanning Lidar Based on a Fast Algorithm for Ray Intersection

Qishu Qian[1,2,3,a], Yihua Hu[1,2,3,b], Nanxiang Zhao[1,2,3,c], Minle Li[1,2,3,d] and Fucai Shao[4,e]

[1]State Key Laboratory of Pulse Laser Technology, Anhui 230037, China;

[2]National University of Defense Technology, Anhui 230037, China;

[3]Anhui Key Laboratory of Electronic Control Technology, Anhui 230037, China;

[4]The Military Representative Bureau of the Ministry of Equipment Development of the Central Military Commission in Beijing, Beijing 100191, China.

[a]creamy777@163.com, [b]skl_hyh@163.com, [c]southfly@163.com,

[d]15555483329@163.com, [e]shaofc_cesec@163.com

Abstract. Due to cost and realistic feasibility limitations, the current research on laser active imaging guidance technology is based on simulation models. In this paper, the complete process of laser emission, target reflection and detector reception are modeled and simulated, and finally the range image is obtained. Due to the large number of actual scene bins, bins are screened first to increase the intersection speed between the beam and the target. Also, a fast algorithm for ray intersection in real scenes is proposed, which improves the operation speed to over 70 times. Based on the fast algorithm, this paper divides the whole imaging process simulation into three steps: beam vector solution, beam target intersection and projection point related information acquisition.

Keywords: 3D laser imaging, point cloud, fast algorithm for ray intersection.

1. Introduction

With high resolution and strong anti-interference ability around the clock, laser imaging [1] is receiving more and more attention. Due to the high research and development cost of lidar, it's too expensive to use missile-borne platform directly, which indicates the necessity of accurate system simulation models [2]. There have been many achievements in the research of lidar simulation at home and abroad [3]. Many foreign research institutions, such as the French Oktal Synthetic Environment Company [4] and the Swedish Defense Research Agency [5], have developed an in-use simulation platform for lidar. Huazhong University of Science and Technology [6] established an airborne dual-wedge laser imaging radar simulation platform, and obtained 3D images in different scenes, but the single-point scanning efficiency is too low. National University of Defense Technology [7] carried out simulation modeling of the scanning lidar. The range images and the intensity images were obtained by analyzing the echo information in each beam, but the working distance was close and the scanning period was too long. At present, there is no simulation of lidar under the missile platform. Using line array scanning lidar to collect 3D data can realize reconnaissance of long-distance targets, and has great prospects in guidance.

The research team is working on the development of the missile-borne linear array scanning lidar. In this paper, the missile-loaded linear array scanning lidar system is simulated, and the performance of the lidar system is evaluated and analyzed, which provides an important reference for the development work. At the same time, the simulated data can be used to carry out related algorithm research.

2. System Simulation and Modeling

The system is composed of a laser, a scanner, a beam splitter, a position and attitude measuring system and a photon receiving unit, with its working principle shown in Fig. 1. The laser emits laser

pulses, which are divided into multiple parallel beams by a beam splitter. The scanning in the vertical direction is driven by the scanning mechanism to perform a reciprocating sweep, and the echo signal is received by the photon detector. Finally, the coordinates are calculated by data processing.

The lidar beam vector is S and $V_s(x_v, y_v, z_v)^T$ is where it starts from. The coordinates can be measured by dynamic differential GPS. The size of S is the distance between the optical system and the ground laser foot, and its attitude parameters (α,β,γ) can be obtained by the high-precision attitude measuring device. According to the above infos, the geodetic coordinates of the ground point P can be solved. The system continuously acquires laser pulses and receives echo information by scanning, and can acquire high-precision laser point cloud data. In order to simulate the working process of linear array scanning laser imaging radar, this paper firstly models the laser emission, laser and target interaction and laser receiving process. In this paper the simulation of the system working process is divided into three parts: the laser emission, laser and target interaction and laser reception.

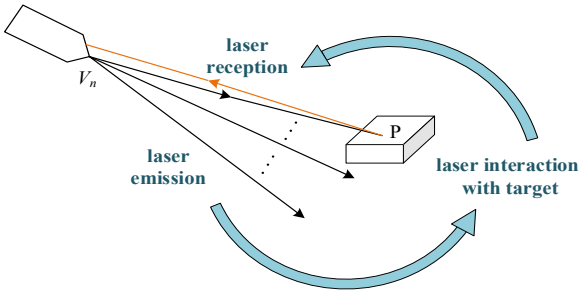

Fig. 1 Schematic diagram of the detection target of the missile-borne line sweep lidar system

2.1 Laser Emission Process Modeling

To simulate the laser emission process, the beam vector is used to represent the directional line between the platform and the center of the laser landing point and is determined by the position, attitude and direction of the missile. Solving the vector is important in the simulation. In the modeling process, both the changes of the above factors over time and multiple coordinate transformations based on the geometric relationship should be considered.

Suppose the initial position of the missile be V_0, with the speed and the direction of its motion known. The coordinate V_n of the missile at the time $t=nt_0$ (t_0 is the laser pulse interval) can be expressed as:

$$(x_{V,\mathrm{n}}, y_{V,\mathrm{n}}, z_{V,\mathrm{n}})^T = [f(n,V_0), g(n,V_0), h(n,V_0)]^T \quad (1)$$

$f(n,V_0)$, $g(n,V_0)$, $h(n,V_0)$ are related to the starting position, motion state, and time of the platform.

Shown in Fig. 2, the scanning instantaneous coordinate system O'-$x'y'z'$ is established. The direction of the 32nd beam of 64 beams is taken as the y' axis, the positive yaw direction is taken as the x' axis, and the direction where the pitch angle becomes larger is the z' axis. The origin O' is the intersection between the y' axis and the plane Oxy of the Cartesian coordinate system O-xyz.

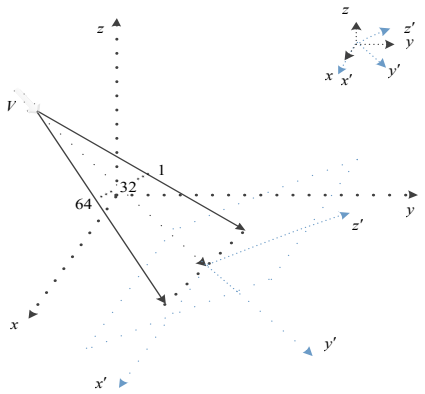

Fig. 2 Cartesian coordinate system and instantaneous scanning coordinate system

The coordinate of the t-time cross-point P between the line laser beam and the plane is:

$$(\mathrm{x}'_{V,\mathrm{n,i}}, \mathrm{y}'_{V,\mathrm{n,i}}, z'_{V,\mathrm{n,i}})^T = \frac{\mathrm{H}_{V,\mathrm{n}}}{\sin(\theta_{V,\mathrm{n}})\cos(\theta_{\Delta,\mathrm{n}})}[\tan(\alpha_i), \tan(\theta_{\Delta,\mathrm{n}}), 0]^T \tag{2}$$

$\theta_{\Delta,\mathrm{n}}$ is the t-time scanning angle of the mirror, α_i is the angle between the 64 lasers and the y' axis and $\mathrm{H}_{V,\mathrm{n}}$ is the t-time height of the platform which equals $z_{v,n}$. $\theta_{V,\mathrm{n}}$ is the t-time depression angle of the platform. Convert the equation (2) from the instantaneous scanning coordinate system to the Cartesian coordinate system:

$$(\mathrm{x}_{V,\mathrm{n,i}}, \mathrm{y}_{V,\mathrm{n,i}}, z_{V,\mathrm{n,i}})^T = \mathbf{T}(\mathrm{x}'_{V,\mathrm{n,i}}, \mathrm{y}'_{V,\mathrm{n,i}}, z'_{V,\mathrm{n,i}})^T + \mathbf{\Delta\omega} \tag{3}$$

The matrix T is a coordinate transformation matrix. The rotation, pitch, yaw angle of the missile platform changes φ_r, θ_P, and ϕ_h, respectively. The matrix $\mathbf{\Delta\omega}$ represents the effect of displacement during the transformation.

$$\mathbf{T} = \begin{bmatrix} \cos(\varphi_r) & -\sin(\varphi_r) & 0 \\ \sin(\varphi_r) & \cos(\varphi_r) & 0 \\ 0 & 0 & 1 \end{bmatrix} \begin{bmatrix} 1 & 0 & 0 \\ 0 & \sin(\theta_P) & -\cos(\theta_P) \\ 0 & \cos(\theta_P) & \sin(\theta_P) \end{bmatrix} \begin{bmatrix} \cos(\phi_h) & \sin(\phi_h) & 0 \\ -\sin(\phi_h) & \cos(\phi_h) & 0 \\ 0 & 0 & 1 \end{bmatrix} \tag{4}$$

$$\mathbf{\Delta\omega} = (x_{V,\mathrm{n}}, y_{V,\mathrm{n}}, 0)^T + (0, \frac{H_0}{\tan(\theta_{V,\mathrm{n}})}, 0)^T \tag{5}$$

Therefore the beam vector can be expressed as:

$$\overrightarrow{PV_{\mathrm{n}}} = \mathbf{T}(\mathrm{x}'_{V,\mathrm{n,i}}, \mathrm{y}'_{V,\mathrm{n,i}}, z'_{V,\mathrm{n,i}})^T + \mathbf{\Delta\omega} - [f(n, V_0), g(n, V_0), h(n, V_0)]^T \tag{6}$$

2.2 Target Reflection Process Based on Fast Intersection

In this paper, not intensity images but range images of the target are received. That's why there is no need to consider the factors affecting the target reflectivity. After finding the beam vector emitted by the laser, the interaction process between the laser and the object can be approximated by calculating the intersection of the beam vector and the target. To get range images of targets, calculating the crossing point of the laser and the target is as effective as to simulate the intersection between the vector and the target. Models used are created by 3DS Max, where model surfaces are consisted of many small triangular facets. So this process is to calculate the intersection between the vector and the facets.

In addition, because a model usually contains a large number of bins, each beam vector and each bin need to be intersected, and then results should be traded off. If the model consists of 1000 bins, one frame image contains 64*500 rays, and the calculated amount of laser projection points will reach $1000 \times 64 \times 500 = 3.2 \times 10^7$. Therefore, it's essential to improve the calculation efficiency of the ray intersection.

Different from the literature [8], there're 64*1 receivers, which can't divide the beam into N sub-beams. Hence, this paper takes the laser beam as a whole. That's why the paper approximated the detection area as a triangle instead of a quadrangular pyramid. In this paper, the line laser observation area is inspected at each scanning dwell position in units of the position where the line

scan is resident. The observation area is a triangle composed of the laser source and the rays of the two edges.

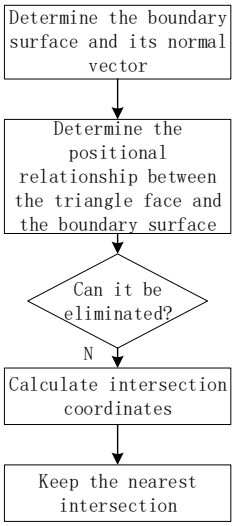

Fig. 3 Design flow of target reflection process simulation

The boundary surface P1 is determined by the position of the laser source V and the direction vector $\overrightarrow{VA},\overrightarrow{VB}$ of the two boundary rays. As P1, P2is determined by $\overrightarrow{VA},\overrightarrow{VC}$ and V, P3 is determined by $\overrightarrow{VB},\overrightarrow{VD}$ and V. Set the normal vectors of boundary surfaces:

$$\begin{aligned}\mathbf{n}_1 &= \overrightarrow{VA}\times\overrightarrow{VB} = \begin{bmatrix} a_1 & b_1 & c_1 \end{bmatrix}^T \\ \mathbf{n}_2 &= \overrightarrow{VA}\times\overrightarrow{VC} = \begin{bmatrix} a_2 & b_2 & c_2 \end{bmatrix}^T \\ \mathbf{n}_3 &= \overrightarrow{VD}\times\overrightarrow{VB} = \begin{bmatrix} a_3 & b_3 & c_3 \end{bmatrix}^T \end{aligned} \tag{7}$$

The normal direction is determined by the vector right-hand rule that when the forward scan is performed, its normal can be determined to point to the direction of the scanning motion. Considering that the actual points only cover part of the scene, that is, the beam intersects only part of the surface of the target. Therefore, bins can be screened first, and only those that may have intersections are retained, which will help improve the computational efficiency of the ray intersection.

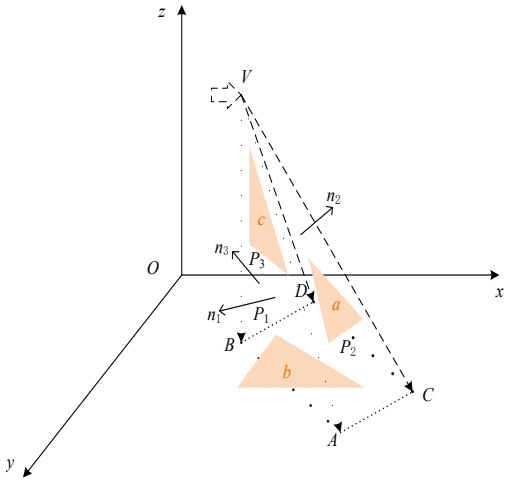

Fig. 4 Schematic diagram of linear array laser observation area

As shown in Fig. 4, two edge landing points A(x_a, y_a, z_a), B(x_b, y_b, z_b) are already known. For the convenience of calculation, auxiliary points C and D are set to $(x_{a+\triangle}x, y_a, z_a)$ and $(x_{b+\triangle}x, y_b, z_b)$, respectively. Due to the ductility of plane P_1, two other planes are constructed to define the excess. Plane VCD is fictitious and its actual observation is limited by P_1. Therefore, there may be only three kinds of positional relationships between bins in the target scene and the observation area of

the laser beam. There're three types of panels, a, b and c shown in Fig.4, which respectively represent the panel is completely in, partly in and completely outside the observation area. Obviously, the last case can be eliminated with no possibility of intersection.

P_1, P_2, P_3 can be expressed by $a_ix+b_iy+c_iz=d_i(i=1,2,3)$.The judgment of the positional relationship between the panel and the laser beam irradiation range can be based on:

$$\mathbf{M}=\begin{bmatrix} x_1 & x_2 & x_3 \\ y_1 & y_2 & y_3 \\ z_1 & z_2 & z_3 \end{bmatrix}^T \begin{bmatrix} a_1 & a_2 & a_3 \\ b_1 & b_2 & b_3 \\ c_1 & c_2 & c_3 \end{bmatrix} - \begin{bmatrix} d_1 & d_2 & d_3 \\ d_1 & d_2 & d_3 \\ d_1 & d_2 & d_3 \end{bmatrix} \tag{8}$$

M(i,j) indicates the positional relationship between *i* and *j*. If the first column in matrix M is all greater or less than zero, then the bin is not intersected with the boundary surface P_1 and can be rejected. The second and the third column in the matrix M respectively represent the positional relationship between the bin and P_2, P_3. If the second or the third column is all greater than zero, *i* is located outside the quadrangular pyramid and can also be eliminated. The conventional algorithm usually calculates the coordinates of all crossing points between remaining bins and rays. Since the occlusion problem of the target itself, for the case where there is an intersection between a certain beam and multiple bins on the target, it is only necessary to keep the intersection closest to the platform.

2.3 Laser Receiving Process Modeling

After obtaining the intersections, the probability of detection of all intersections need to be known. By setting a reasonable threshold, the point which its probability reaches the threshold is displayed to obtain the final range image. The influence factors of the detection probability mainly include the distance from the laser source, the target reflectivity, the atmospheric transmission and so on. Compared with the power consumption of the linear detection system of several hundred watts, the lidar using the photon counting system can achieve the mission requirements with lower laser power consumption with higher feasibility, and is more suitable for long-distance fast 3D imaging. Based on the photon counting detection system, the probability density distribution of the discrete stochastic process output by the photon counting detector is as equation9:

$$p_{sn}(k)=\frac{\exp(-NK_n)}{(K_s+1)^N(N-1)!}\sum_{j=0}^{\infty}\frac{(NK_n)^j}{j!}\frac{(k+N-j-1)!}{(k-j)!}\left(\frac{K_s}{K_s+1}\right)^{k-j} \tag{9}$$

K_s is the average of the counts in the time interval. K_n represents the mean value of the noise count value in the count interval, and N is the count interval. The detection probability [8] can be expressed as:

$$PD=P(k>K_{th})=\sum_{K_{th}}^{\infty}p_{sn}(k)=1-\sum_{0}^{K_{th}}p_{sn}(k) \tag{10}$$

3. Experimental Results and Analysis

Simulation conditions: The platform is set as a missile. The distance from the target scene origin to the platform is 3000*m*. The moving speed is 1 Mach, the rotation speed is 1*r/s*, the elevation angle of the laser beam center direction is 30° with respect to the target scene coordinate system, and the azimuth angle is 0°. The parameters of the lidar system simulated in this paper are as follows: re-frequency 10*KHz*, frame rate 20*Hz*, Therefore, a maximum of 64*500 points can be obtained for each frame range image, and the divergence angle of the laser is 0.5 *mrad*.

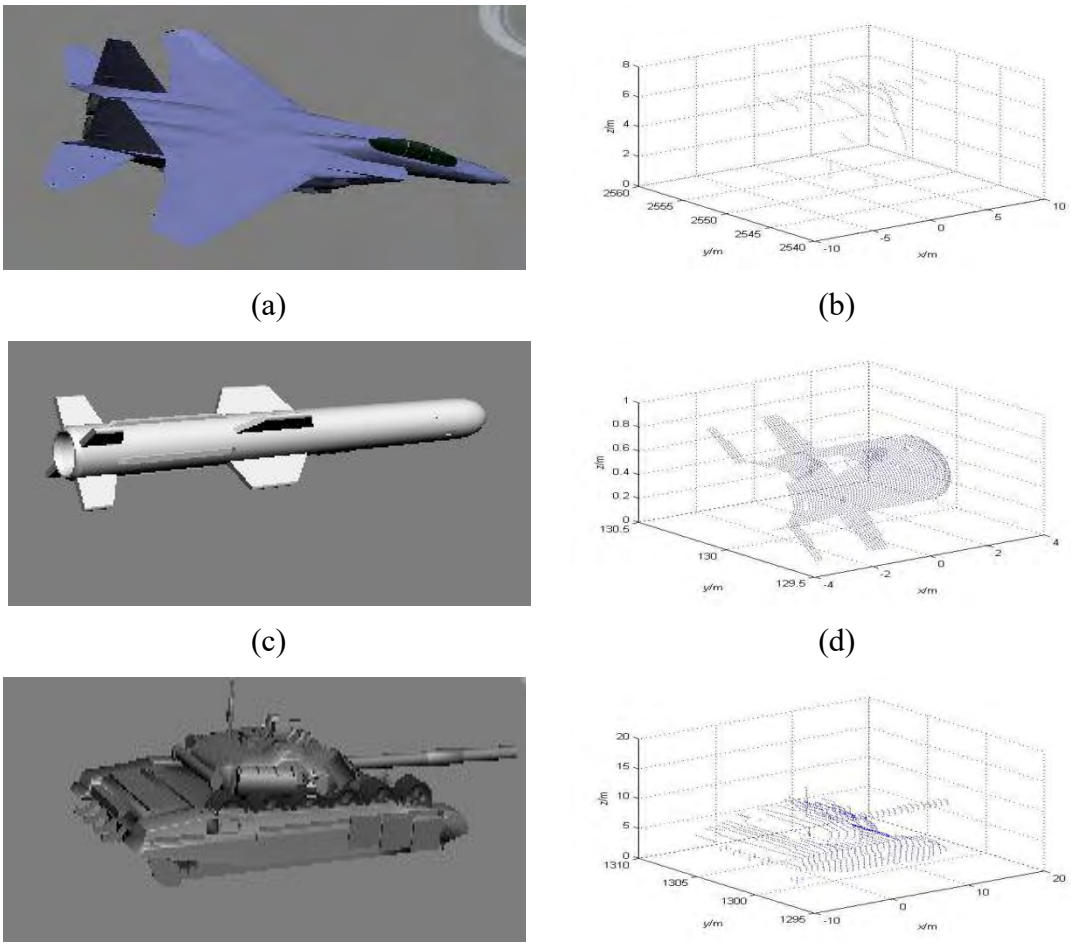

Fig. 5 Different 3D model simulation results. (a) aircraft model; (b) aircraft point cloud image;(c) missile model;(d) missile point cloud image; (e) tank model; (f) tank point cloud image

Firstly, the model established in this paper is verified by single object models. (a), (c) and (e) in Fig. 5 are models simulated by 3DS MAX. (b), (d), and (f) are the corresponding range images obtained from the simulation. In this paper, the linear array scanning laser used in this paper has a high repetition frequency, so range images are composed of strip-shaped dense laser falling points. The occlusion only retains the first intersection, so only models at a certain angle are displayed. The sparseness of the drop points in the obtained range map differs from the number of faces constituting the model. From the above, it can be judged that the simulation system proposed in this paper is feasible.

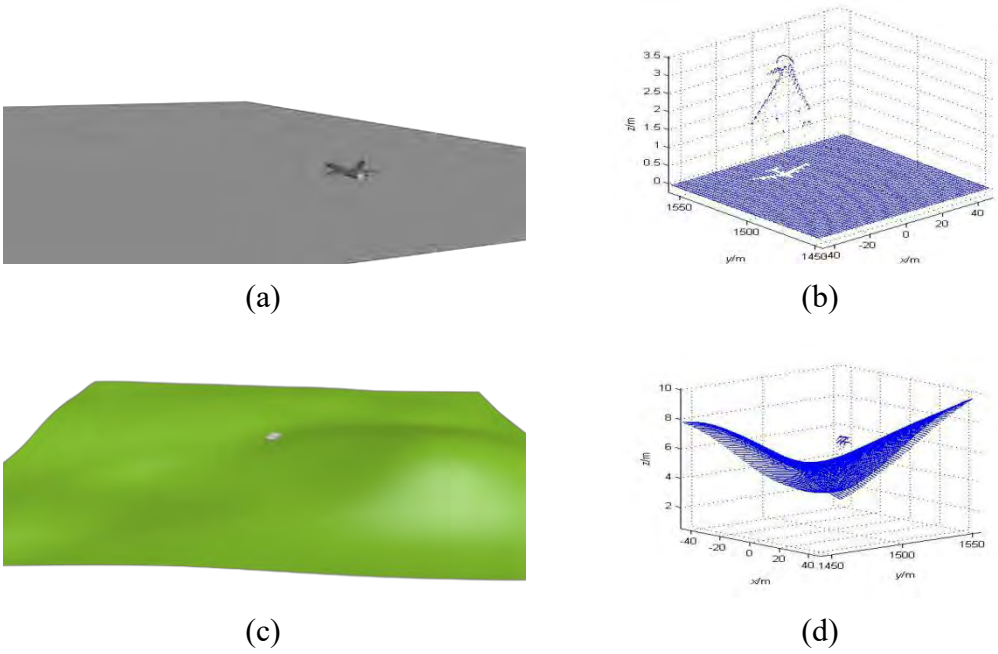

(a) (b)

(c) (d)

Fig. 6 Different 3D scene simulation results. (a) an airplane parked on a flat ground; (b) a point cloud image corresponding to a scene; (c) a vehicle traveling in a bumpy mountain; (d) a point cloud image corresponding to the scene

Table 1 Time consumption comparison of different 3D models

models	total surface element	Baseline 1 time/s	Baseline 2 time/s	proposed algorithm time/s
F15EL	9415	486095	7595	42
missile	12970	674177	10534	53
T72tank	14562	849731	13277	77
mountain	34021	934008	14594	205
airport	5904	349756	5465	45

To verify the effect of the proposed fast intersection algorithm, two methods, recorded as Baseline1 and Baseline2 respectively, are used to generate range images. Baseline1 performs an intersection operation with all bins in the scene in order of sequence numbers 1 to 64 for the 64 beam vectors of each scan, and obtains 64 intersection coordinates. In contrast, Baseline2 uses a parallel computing strategy to simultaneously perform the intersection of 64 beam vectors and the target scene to obtain 64 intersection coordinates. Obviously, the above two algorithms do not filter the bins before the intersection operation, so a huge amount of computation will be generated.

It can be seen from Table 1 that the proposed algorithm is up to 11,633 times larger than Baseline1, and the average can reach 9546 times. Compared with Baseline2, the proposed algorithm is up to 199 times, and the average is 148 times. Obviously, Baseline2 is about 64 times faster than Baseline1 because of the parallel intersection. The smaller the total number of bins, the more the speed increases.

Since Baseline1 and 2 perform the same operation for all bins, the proposed fast algorithm considers the area composed of 64 laser beams as a whole, and screens the bins that may have intersections, thus reducing computation for the intersection of rays. Therefore, using the fast algorithm can significantly reduce the time for the intersection of the laser beam and the target

scene model. That's to say, the proposed fast algorithm of ray intersection based on the spatial boundary of laser beam has higher computational efficiency and better stability.

4. Summary

In order to carry out the actual experiment of the missile-loading platform, this paper firstly proposes a laser-borne linear array scanning lidar imaging model based on the beam fast intersection algorithm. The model simulation of the linear array lidar is decomposed into three steps, and the scene and individual objects are scanned by the fast intersection algorithm to obtain range images. For a single object, the algorithm can run for less than 60 seconds. For larger scenes, the running time is about 200 seconds. And compared to the traditional algorithm, its running speed can be increased by several dozen times. Through simulation, this paper provides a theoretical basis for the development of the actual missile system. At the same time, data obtained through simulation can be used for the research of the point cloud target tracking recognition algorithm in the future.

Acknowledgements

This work was financially supported by Chinese National Natural Science Foundation (61271353, 61871389).

References

[1]. Snyder M, Qu Z, Hull R, et al. Quad-segment polynomial trajectory guidance for impact-time control of precision-munition strike. IEEE Transactions on Aerospace and Electronic Systems.Vol. 52(2016) No.6, p. 3008-3023.

[2]. Han Y,Sun H Y,Li Y C, et al. Advances in foreign simulation softwares of imaginglidar. Laser & Optoelectronics Progress. Vol. 50(2013) No.1,p. 46–54.

[3]. Douchin N, JOLY A, Meynard T, et al. Simulation of active EO imagine system based on SE Workbench and OSMoS software tools.5th international lR Target and Background Modeling & Simulation Workshop. 2009, p. 1-18

[4]. Chevalier, Tomas R, Steinvall, et al. Laser radar modeling for simulation and performance evaluation.International Society for Optics and Photonics. 2009,p. 748206.

[5]. Wu X G: Study of moving target detection and recognition based on lidar(postgraduate, Huazhong University of Science and Technology,China 2015). p. 12-15.

[6]. Chen X: Research on target feature extraction and recognization based on imaging ladar(postgraduate, National University of Defense Technology, China 2015).p. 18-19.

[7]. Chen X, Shi Z G, Yang W P, et al. A fast simulation algorithn of scanning lidar. CHINESE JOURNAL OF LASERS. Vol. 41(2014) No.8, p. 0814002.

[8]. Zhao M B, He J, Fu Q. Simulation modeling and analysis of full-waveform ladar signatures. ACTA OPTICA SINICA. Vol. 32(2012) No.6,p. 06280.